Dynamics of hydrated proteins and bio-protectants: caged dynamics, β-relaxation, and α-relaxation

K.L. Ngai[a*], S. Capaccioli[a,b], A. Paciaroni[c],

[a]*CNR-IPCF, Largo Bruno Pontecorvo 3 ,I-56127, Pisa, Italy*

[b]*Dipartimento di Fisica, Università di Pisa, Largo Bruno Pontecorvo 3 ,I-56127, Pisa, Italy*

[c]*Dipartimento di Fisica, Università degli Studi di Perugia, Via A. Pascoli 1, 06123 Perugia, Italy*

* Corresponding author. Email addresses: kia.ngai@pi.ipcf.cnr.it , kiangai@yahoo.com

ABSTRACT

BACKGROUND: The properties of the three dynamic processes, alpha-relaxation, nu-relaxation, and caged dynamics in aqueous mixtures and hydrated proteins are analogous to corresponding processes found in van der Waals and polymeric glass-formers apart from minor differences.

METHODS: Collection of various experimental data enables us to characterize the structural alpha-relaxation of the protein coupled to hydration water (HW), the secondary or nu-relaxation of HW, and the caged HW process.

RESULTS: From the T-dependence of the nu-relaxation time of hydrated myoglobin, lysozyme, and bovine serum albumin, we obtain T_{on} at which it enters the experimental time windows of Mössbauer and neutron scattering spectroscopies, coinciding with protein dynamical transition (PDT) temperature T_d. However, for all systems considered, the alpha-relaxation time at T_{on} or T_d is many orders of magnitude longer. The other step change of the mean-square-displacement (MSD) at T_{g_alpha} originates from the coupling of the nearly constant loss (NCL) of caged HW to density. The coupling of the NCL to density is further demonstrated by another step change at the secondary glass temperature T_{g_beta} in two bio-protectants, trehalose and sucrose.

CONCLUSIONS: The structural alpha-relaxation plays no role in PDT. Since PDT is simply due to the nu-relaxation of HW, the term PDT is a misnomer. NCL of caged dynamics is coupled to density and show transitions at lower temperature, T_{g_beta} and T_{g_alpha}.

GENERAL SIGNIFICANCE:

The so-called protein dynamical transition (PDT) of hydrated proteins is not caused by the structural alpha-relaxation of the protein but by the secondary nu-relaxation of hydration water.

1. BACKGROUND

Hydrophilic glass-formers are miscible with water and the aqueous mixtures can be studied over some range of concentration without crystallization. The choice of the glass-formers include hydrazine (N_2H_4) and other small molecules with hydrogen bonding [1-3], ethylene glycol and its oligomers and polymer, propylene glycol and its oligomers, glycerol and polyalcohols [4-9], poly(vinylpyrrolidone) (PVP) [10-15], poly(2-hydroxyethylmethacrylate) [16,17], the monosaccharides [10, 18], and the disaccharides [19-21], some of which are bio-protectants. From the experimental data of our own and others, three major processes are delineated by analyzing the isothermal dielectric spectra on cooling from temperatures above the glass transition temperature T_g and down to temperatures way below it. The structural α-relaxation, the slowest of all processes, appears prominently in the dielectric loss spectra at temperatures above T_g. At higher frequencies/lower temperatures than the α-relaxation is the faster secondary relaxation originating from the water component. Several names have been given to it including the ν-relaxation [4] (from the Greek word 'νερο' for water), the Johari-Goldstein (JG) β-relaxation of the water component [5], and the water-specific secondary relaxation [7]. The term, JG β-relaxation, was used because the ν-relaxation shares some properties of secondary relaxation in many glass-formers classified as such [22, 23]. In fact, the purpose of the publications [5, 7] was to demonstrate that the water-specific secondary or ν-relaxation in aqueous mixtures shares many properties of the JG β-relaxation of common glass-formers, which had not been done before.

Even faster than the ν-relaxation is the caged molecules dynamics, which appear as the nearly constant loss (NCL) in the dielectric spectra at low temperatures. In this case, the dielectric loss $\varepsilon''(f)$ data exhibit the frequency dependence, $\varepsilon''(f) \propto f^{-c}$ with c positive and significantly less than 1, at frequencies higher than f_ν, the frequency of the ν-relaxation, and temperatures below and above T_g. The NCL of caged dynamics was seen in a few dielectric studies of aqueous mixtures, where measurements were made at sufficiently low temperatures [2, 3]. This NCL is generally found in dielectric relaxation of all molecular glass-formers [24-26], and is interpreted as the loss from molecules while caged by the anharmonic intermolecular potential at short times before the onset of the JG β-relaxation.

3

The properties of the three relaxations, α-relaxation, ν-relaxation, and caged dynamics (NCL) in aqueous mixtures and hydrated proteins are analogous to corresponding processes found in van der Waals and polymeric glass-formers, and binary mixtures. There are, however, minor differences, because water molecules have a small size and are effective in hydrogen bonding. A summary is given as follows.

(*i*) The ν-relaxation has the characteristics of the Johari-Goldstein β-relaxation in non-aqueous glass-forming systems [22, 24]. For example, its relaxation strength $\Delta\varepsilon_\nu$ is a monotonically increasing function of temperature below and above T_g, and $\Delta\varepsilon_\nu$ as well as its relaxation time τ_ν change T-dependence on crossing T_g similar to the same quantities of the faster component in binary mixtures of van der Waals glass-formers, and in pure glass-formers. Also τ_ν and $\Delta\varepsilon_\nu$ are dependent on the molar concentration of water and the molecular weight of the solute. All these properties are indicating that the ν-relaxation and the α-relaxation are coupled, like the Johari-Goldstein (JG) β-relaxation in van der Waals and polymeric glass-formers. However the ν-relaxation in aqueous mixtures and hydrated proteins ~~is a special kind of~~differs from the JG β-relaxation of the conventional glass-formers because of two properties. Firstly, water molecules cannot only rotate but can also translate after breaking two hydrogen bonds, unlike the absence of translation in many conventional glass-formers. Secondly, the ν-relaxation arises from the water component of the binary mixture, while the JG β-relaxation in conventional glass-formers arises from the same molecules that generate the α-relaxation.

(*ii*) On increasing water content, and as long as the mixture remains in the glassy state (i.e. $T < T_g$), τ_ν decreases due to diminishing coupling of water to the solute. This behavior of the ν-relaxation is similar to the decrease of the α-relaxation time of the faster component in binary mixtures of glass-formers on increasing the content of the faster component [27, 28]. Notwithstanding, there is a difference by the fact that the decrease of τ_ν is towards the Arrhenius temperature dependence, defined approximately by $\hat{\tau}_\nu(T) = \tau_\infty \exp(E_a/RT)$ with $\tau_\infty = 10^{-17}$s and E_a=50 KJ/mol. At sufficiently high concentration of water, the limit $\hat{\tau}_\nu(T)$ is more or less reached by $\tau_\nu(T)$, independent of the solute in the aqueous mixtures. This trend reflects decoupling of the ν-relaxation from the solute, supported by the fact that $\hat{\tau}_\nu(T)$ is almost the same as the relaxation time of water subjected to nano-confinement and prevented from crystallization [7].

4

(*iii*) In most aqueous mixtures, the α-relaxation time, τ_α, with the Vogel-Fulcher-Tammann (VFT) temperature dependence decreases more rapidly than τ_ν, resulting in merging of the two relaxations when at some temperature above T_g [5]. However there are exceptions which has τ_α several decades longer than τ_ν at temperatures where τ_ν is approaching 100 ps. Examples include the mixture of polyvinylpyrrolidone (PVP) with 40 wt.% water [10, 15], and several hydrated proteins to be discussed separately later.

(*iv*) The magnitude of the NCL of caged dynamics changes from a weaker temperature dependence below T_g to a stronger one above T_g. This property indicates that the NCL is sensitive to glass transition, density dependent, and coupled to the α-relaxation. Dielectric data at frequencies below 1 MHz showing this property in a few aqueous mixtures can be found in Ref.[2], and in many glass-formers with and without hydrogen bonds [24,26,29,30]. Incoherent neutron scattering and dynamics light scattering have the advantage of probing dynamics at time scales shorter than typically 1 ns. Certainly at temperatures below T_g and in some limited range above T_g, the caged dynamics are the only processes probed (other than vibrations and methyl group rotation) because τ_α and τ_ν are much longer than 1 ns. The property of NCL was generally observed in terms of the mean square displacement, $<u^2(T)>$, in a variety of glass-formers by neutron scattering [31], and in terms of quasielastic intensity by high frequency light scattering [25,29,32,33]. An example of the property of NCL from neutron scattering in aqueous mixtures can again be taken from $<u^2(T)>$ of PVP with 40 wt.% water [10].

Based on the insights into the three major processes in aqueous mixtures described in the above, we ventured into the study of the dynamics of hydrated and solvated proteins, expecting similar properties will be observed [10, 21]. The dynamics of interest are in the hydration and solvation shell and the protein it couples to. The configuration in hydrated and solvated proteins is thus different from bulk aqueous mixtures and we can expect some differences or new effects not found generally in aqueous mixtures. The objective of this regular article is to bring out results of the dynamics of hydrated proteins from measurements of our own as well as from others. The combination of the data from broadband dielectric relaxation, neutron scattering, and calorimetry are used to differentiate some of the interpretations of the dynamics of hydrated proteins, and evaluate their validity. Furthermore, the dynamics of the bio-protectants, sucrose and trehalose, are included in the discussion, because their dynamics are relevant for consideration of the proteins embedded in the bio-protectants.

2. METHODS

Literature ~~and our own~~ data from studies by dielectric relaxation, calorimetry, and nuclear magnetic resonance on the dynamics of hydrated proteins are assembled together to characterize the various molecular processes present and evaluate their relevance to the so called 'protein dynamics transition' (PDT) observed by Mössbauer spectroscopy and neutron scattering. The term PDT in literature usually stands for the step change in temperature dependence of either the mean square displacement or the elastic neutron scattering intensity at a temperature usually designated by T_d. The proteins considered include myoglobin, lysozyme, and bovine serum albumin at different hydration levels. The same consideration is given to the molecular dynamics of a mixture of polyvinylpyrrolidone (PVP) with 40 wt.% of water. The purpose of this is to show that the dynamics found by dielectric relaxation, calorimetry, and nuclear magnetic resonance are similar to hydrated proteins, exactly the same properties of PDT is observed although there is no protein in the hydrated PVP.

Using the rich spectroscopic information on the dynamics of hydrated protein amassed, we determine which observed relaxation, the structural α-relaxation or the HW secondary or ν-relaxation is responsible for the PDT. If the α-relaxation is the origin, then the thesis proposed by Doster et al. [34-36] is verified, and the term PDT at T_d is justified. On the other hand, if the ν-relaxation is the origin, then the effect is simply the ν-relaxation entering at some temperature the time window accessible to Mössbauer or neutron scattering spectroscopy, and the term PDT is a misnomer. Moreover, a two-step scenario for the protein dynamical transition has been proposed [35, 36] based on the mode coupling theory (MCT). The first step is the fast β-process for caging in MCT [37]. We shall use experimental data to tell whether it has any validity or not.

As we have pointed out before, there is a step increase (decrease) of the mean square displacement (elastic intensity) at the glass transition temperature T_g independent of the energy resolution of the neutron scattering spectrometer [10, 21, 38]. This effect originates from the response of the caged HW, exhibiting as the nearly constant loss (NCL) in susceptibility. Although the effect as well as the NCL is general and found in all glass-formers, the NCL of

6

hydrated protein has not been seen before, with just an exception. We found it in a recently published dielectric relaxation study of hydrated lysozyme [39]. The dynamics of bio-protectants such as the saccharides are related to that of the protein embedded in the bio-protectant [42]. The mixture of polyvinylpyrrolidone (PVP) with 40 wt.% of water has shown all the properties of hydrated proteins.

Recent study of the caged dynamics and NCL by terahertz absorption spectroscopy and neutron scattering of polyalcohols, pharmaceuticals, polymers, and van der Waals molecular glass-formers have found the caged dynamics respond by change not only at the nominal $T_{g\alpha}$ but also at the secondary glass transition $T_{g\beta}$ [41-44] much lower than $T_{g\alpha}$. It would be interesting to find the same in the bio-protectants. For this reason, we analyse dielectric relaxation and neutron scattering data of trehalose and sucrose to search for the effect.

3. RESULTS

(A) Hydrated Myoglobin, Lysozyme, and Bovine Serum Albumin

With the insights into the ν-relaxation and caged dynamics gained from the study of aqueous mixtures, we explore the dynamics of hydrated proteins. The objectives are twofold. One is to look for the ν-relaxation and caged dynamics in hydrated proteins and see if they have the properties (*i*)-(*iv*) found in aqueous mixtures. The other is to characterize the α-relaxation and the ν-relaxation in hydrated proteins, and to determine which one is responsible for the protein dynamic transition (PDT) [34-36, 45-47]. In many aqueous mixtures [4,5,7], τ_ν merges with τ_α at high frequencies of Mössbauer spectroscopy and neutron scattering used to probe the dynamics of hydrated proteins and in particular the PDT. If this happens also in hydrated proteins, then one can say that it is the α-relaxation that causes the PDT, as proposed by some authors in literature [34-36].

However, there are exceptions. An example is hydrated PVP mentioned before [10,15]. As shown in the inset of Fig.1, its τ_ν remains much shorter than τ_α at any of the short time-scales of Mössbauer spectroscopy and neutron scattering. The glass transition at $T_g \approx 216$ K from DSC

measurement is indicated by the dashed line. The red line is the VFT fit of the τ_α data with parameters given in ref.[15], which reaches 100 s at T=218 K and 1000 s at T=216.7 K close to the DSC $T_g\approx$216 K. From this, it is clear that τ_α is the structural α-relaxation time of the PVP in aqueous mixture, but not τ_v at all.

The main part of Fig.1 shows the mean square displacement $<u^2>$ from neutron scattering changes T-dependence first at T_g~216 K, and then at the PDT temperature, T_d~260 K. Recognized by many is a lower T_d is found for the same hydrated biomolecule from the MSD obtained by spectrometer having a longer observation time window. This trend is particularly clear when considering the much lower T_d found by Mössbauer spectroscopy [48] than by neutron scattering. The former has resolution time of 140 ns much longer than any quasielastic neutron scattering spectrometers. An example of the trend from neutron scattering data can be taken from the 2010 paper by Jasnin et al. [49] obtained by three spectrometers, IN6, IN13, and IN16, on three different time scales of 10 ps, 100 ps, and a few ns respectively, and was explained by the so-called 'frequency-window model' in the 2008 paper by Becker et al. as an instrumental energy resolution effect [50]. The effect suggests that the increase of the MSD on increasing T past T_d is caused by a relaxation process entering the longest time scale t_{exp} in the time window of the instrument. In the Philos. Mag. paper from our group first published in 2010 [51], we found good correspondence between the experimental value of T_d and the estimate of T_d from the temperature at which the ν-relaxation time, τ_v, of hydration water is comparable to (or exceeding by a few times) t_{exp} of the spectrometer used in the measurement. In the book published in 2011 [33] to be followed by the 2012 paper [21], many more published data from neutron scattering and Mössbauer spectroscopy, the estimated T_d from the empirical criterion, $\tau_v \approx t_{exp}$, are in good agreement with experimental value. In 2011, Magazù and coworkers [52] performed different neutron scattering experiments with different instrumental energy resolutions on dry and hydrated lysozyme. From their results, they showed the PDT is indeed a finite instrumental energy resolution effect, and it appears when the characteristic system relaxation time intersects the resolution time of the instrument. At the same year, Magazù and coworkers [53] formulated the resolution elastic neutron scattering (RENS) method, with specific reference to the temperature-relaxation time-instrumental resolution-crossing point. This method is further elaborated in a review in ref.[54]. Thus the RENS method of Magazù and

coworkers provides a formalism for justification of our empirical criterion, $\tau_\nu \approx t_{exp}$, used before [21,33,51] to locate T_d. The approach of Magazù and coworkers which is consistent with ours is applied in the present paper to analyze the MSD data in Fig.1 and figures to follow up to Fig.5. In passing, we mention also According to an another empirical rule proposed by Doster in 2008 [46], which states that if the relaxation process has a Lorentzian shape, the onset of the transition at T_d occurs when $\tau_{res}=0.2\tau_{max}$, where τ_{max} is the most probable time of the relaxation process and τ_{res} is the longer experimentally accessible timescale.

The energy resolution ΔE (full width at half maximum) of the neutron spectrometer is approximately linked to the longest measurable characteristic time τ_{res} by the relationship $\tau_{res}(ps)$ ~1316/$\Delta E(\mu eV)$ [21]. Applying this to the QENS spectrometers used at the Institute Laue-Langevin, we calculated log(τ_{max}/s) for IN6, IN13, and IN16 (whose typical nominal energy resolutions are 90 μeV, 9 μeV and 1 μeV respectively) to be -10.14, -9.14, and -8.18 respectively. Alternatively, direct matching at the crossover temperature T_d, i.e. $\tau_{res}=\tau_{max}(T_d)$, gives log($\tau_{max}(T_d)$/s) for IN6, IN13, and IN16 to be -10.84, -9.84, and -8.88 respectively, while for Mössbauer spectroscopy [48-5055-57], we get log(140×10^{-9}/s)=-6.85. The neutron scattering $<u^2>$ of hydrated PVP were measured at the IN16 spectrometer. In the inset of Fig.1 and at T_d ~260 K, from the various sources of data, logτ_ν assumes the value of ranging from -8.2> logτ_ν >-9, about the two values for IN16. Therefore the change at T_d ~260 K observed in hydrated PVP is due to the ν-relaxation, and definitely not due to the α-relaxation, because τ_α at T_d~260 K is about 3 decades longer than $\tau_\nu \sim \tau_{res}$. The onset of increase of $<u^2>$ or equivalently the decrease of the elastic scattering intensity at T_d in hydrated PVP is simply the effect of the ν-relaxation entering the time window of IN16, and is not related to the α-relaxation and viscous flow at T_d (260 K > T_g=216 K) and the ns time-scale of the neutron scattering spectrometer.

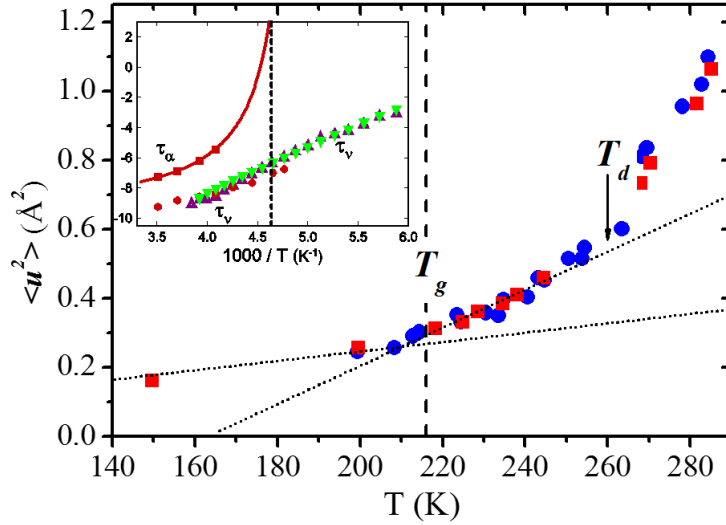**Figure 1.** Mean squared displacement $<u^2>$ in Å^2 obtained from the elastic fixed window scans in QENS experiments on the PVP/D$_2$O (red squares) and the PVP/H$_2$O sample (blue circles). The two lines, same as that given in Ref.[10], bring out the transition at T_g. Original data are from Ref.[15]. The vertical arrow indicates approximately the onset of the change in temperature dependence of $<u^2>$ at $T_d \sim 260$ K. The inset shows τ_α (red squares) and τ_ν (red circles) obtained from neutron scattering at $Q=1$ Å^{-1}. Green inverted triangles: maximum of the Cole-Cole distribution of the "strong" dielectric ν-relaxation. Blue triangles: Cole-Cole relaxation times obtained from spin-lattice relaxation measurements. Red line is the VFT fit to τ_α, and the vertical line indicated the location of mean value of $1000/T_g$ from DSC.

Before returning to discuss hydrated proteins, worthwhile to point out in the inset is the change from Arrhenius dependence of τ_ν at temperatures below T_g to a stronger T-dependence above T_g. This property is found in all aqueous mixtures [4,5,7,14] as well as the JG β-relaxation of neat glass-formers [33], and a component in binary mixtures of glass-formers [27,28]. Also at temperature below T_g and over some range above T_g, even τ_ν is about 3 decades longer than τ_{res}. Therefore, $<u^2>$ has to be contributed by the caged water dynamics, and its change in temperature dependence on crossing T_g reflects the coupling of the caged dynamics to density. Since τ_{res} of other neutron scattering spectrometers usually employed to measure mean squared displacements is either comparable to or shorter than IN16, the caged dynamics is the mechanism probed in a temperature range across T_g by any of the spectrometers used. Hence the

change of temperature dependence of $<u^2>$ at T_g is observed, independent of the energy resolution of the spectrometers. Again this property is generally found in glass-formers of different classes [31], and in hydrated proteins, and proteins solvated by polyalcohols and monosaccharides [10, 21, 38]. Notwithstanding, this property is relatively unknown and often overlooked in the interpretation of $<u^2(T)>$ or elastic intensity of hydrated and solvated proteins. For this reason, our papers [10, 21, 38] were written to show its presence in many systems and revitalize the interest for it. This property of the crossover of $<u^2>$ at T_g has been shown also from neutron scattering data of perdeuterated C–PC, a light harvesting, blue-copper protein, hydrated with 0.3 g/g H_2O in a paper published in 2011 [35]. Notwithstanding, this property is much more general for glass formers as pointed out by one of us in the 2000 review [31]. We further showed the occurrence of this phenomenon in hydrated [38] and solvated [21] proteins. There is also a difference between our interpretation of this property and that provided in literature invoking the mode coupling theory [37] and the two-step decay in the density correlation function. The fast local motions within the cage of nearest neighbors give rise to a fast β-process on a pico-second time scale, while the slow α-process consists of escape out of the cage and long range diffusion. However, the mode coupling theory is valid only at temperatures above the critical temperature, T_c, which is typically about 1.2 T_g. On the other hand, we interpret the fastest dynamics as the NCL of molecules caged by the anharmonic intermolecular potential, which is terminated by the onset of the JG β-relaxation. In turn, the JG β-relaxation is the precursor of the α-relaxation. The evolution of dynamics with time in the order of the NCL, the JG β-relaxation, and the α-relaxations, lead to connections between their properties [33].

Hydrated Myoglobin

Returning to the problem of PDT in hydrated proteins, the discussions above imply two possible scenarios. The first scenario is that the ν-relaxation has already merged with the α-relaxation at the time scale of 140 ns in Mössbauer spectroscopy and *a fortiori* at shorter time scale of τ_{res} in neutron scattering. In this case, after the first step change at T_g, the second step change of $<u^2>$ at T_d is contributed by the α-relaxation and viscous flow as proposed by Doster [34-36]. If this is the case, the nomenclature, PDT, for the second step is meaningful because it is in accord with

the definition given in refs. [34-36]. Appearing in the Abstract of Ref. [34], the definition is given by "*The protein dynamical transition, identified from elastic neutron scattering experiments by enhanced amplitudes of molecular motions exceeding the vibrational level [1], probes the α-process on a shorter time scale. The corresponding liquid-glass transition occurs at higher temperatures, typically 240 K.*". This definition is reinforced in the Abstract of Ref.[36] by "*Our method predicts the protein dynamical transition (PDT) at T_d from the collective (α) structural relaxation rates of the solvation shell as input. By contrast, the secondary (β) relaxation enhances the amplitude of fast local motions in the vicinity of the glass temperature T_g.*".

The second scenario is that the ν-relaxation and the α-relaxation of the hydrated protein behave like that of hydrated PVP in the inset of Fig.1. Then, the second step change of $<u^2>$ has to be identified with the ν-relaxation and the temperature T_d is that at which $\tau_\nu(T_d)$ starts to enter the experimental time window of Mössbauer or neutron scattering spectroscopy. The much slower α-relaxation can possibly contribute to a third step change but at a higher temperature, which may not be reached either because to avoid melting or unfolding of the protein, or simply because the purpose of the experiment is to observe the so called PDT and the second step change is mistaken as it. If the second scenario holds, the second step has nothing to do with the α-relaxation, and it is not the PDT as defined by Doster.

As a support for the 1st scenario, i.e. that the α-relaxation is solely responsible for the second step observed in Mössbauer and neutron scattering spectroscopies, Doster collected together the relaxation times of myoglobin HW from neutron scattering, Mössbauer spectroscopy, iso-frequency specific heat spectroscopy, and part of the dielectric relaxation, and associated all of them with the structural α-relaxation time τ_α [34]. This collection is shown in Fig.3 of ref. [34], and is effectively the same as the inset of Fig.2 reported herein.
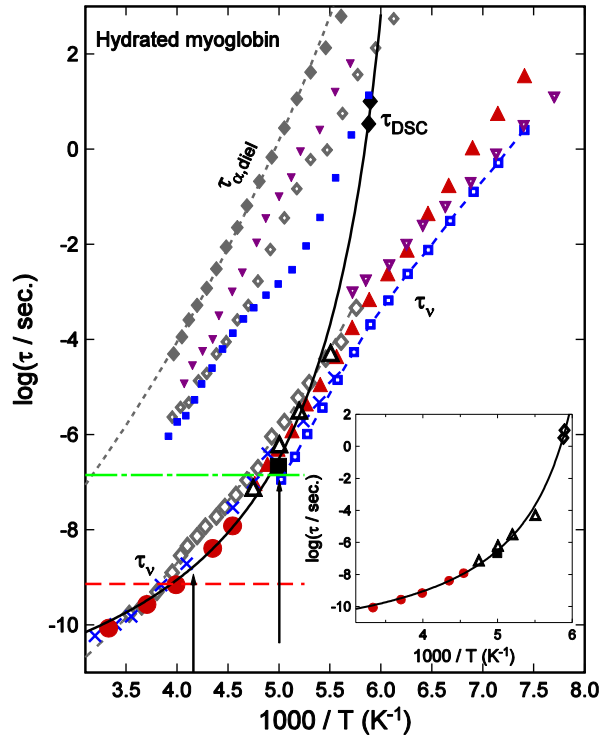
Figure 2. The inset is basically a reproduction of Fig.3 by Doster in Ref.[34], which is the Arrhenius plot of data called the α-relaxation rate $k_S \equiv 1/\tau_\alpha$ for hydrated myoglobin (HW) at $h=0.4$ The red closed circles are from neutron scattering, open black triangles are dielectric relaxation data taken from ref.[~~51~~58], the lone large closed square is from Mössbauer spectroscopy [45], the two open diamonds at the top are from specific heat spectroscopy [34]. The fit to a VFT-equation provided in ref.[34] is also shown (full line). The same symbols as in Fig.3 of this reference are used to represent the relaxation time data of HW. These same data appear also in the main part of the figure. Added are the dielectric τ_ν and τ_α of hydrated myoglobin (purple inverted open and closed triangles respectively) [~~52~~59]. Open blue squares are dielectric τ_ν of hydrated myoglobin at hydration level of $h=0.33$ [~~53~~60]. The NMR relaxation times of hydrated myoglobin at $h=0.35$ are represented by the multiplication signs [~~54~~61]. All other grey color diamond symbols are the three processes found most recently [39]. The arrows are explained in the text.

The line is the fit by a Vogel-Fulcher-Tammann (VFT) equation. However, the collection in ref.[34] considered only the faster dielectric relaxation but ignored the slower relaxation reported by Jansson et al. of hydrated myoglobin at hydration levels of $h=0.80$ [~~51~~58, ~~52~~59] and $h=0.33$

13

[5360] at temperatures above T_g. These slower dielectric process not included in the collection could be the α-relaxation or related to it, and its relaxation times are reproduced in the main part of Fig.2 herein. Shown also are the faster relaxation selected in ref.[34], and considered by Doster as the α-relaxation The VFT fit of the collection of data in ref.[34] are included as well. We put back the dielectric relaxation times with Arrhenius dependence at temperature below T_g of Jansson et al., which have to be identified with τ_ν, but were not considered in ref.[34]. This is in accord with the perception of the author of ref.[34] that the ν-relaxation has already merged with the α-relaxation at temperatures above T_g, and hence the τ_ν data below T_g have no bearing on the PDT and can be ignored. The relaxation times τ_{NMR} from NMR study by Lusceac et al. [5460] at temperatures above and below T_g are also included in Fig.2.

A more definitive identification of the α-relaxation distinctly different and much slower than the ν-relaxation in hydrated myoglobin at h=0.34 is provided by the very recent dielectric measurements by Nakanishi and Sokolov (NS) [39]. Three processes were found and their relaxation times are represented by grey diamonds in Fig.2. The fastest process has relaxation times following closely the dielectric relaxation times of Jansson et al. [5158-5360] as well as τ_{NMR}. NS agreed with us [10,21,38] that it is the analogue of the ν-process observed in many aqueous mixtures because it shares the characteristic properties including change to a stronger temperature dependence of its relaxation time on crossing T_g from below, and its relaxation strength Δε increases with increasing temperature. The intermediate process has relaxation time quantitatively close to the conductivity relaxation time, $\sim\varepsilon_0/\sigma_{dc}$, and the discussion of its origin can be found in Ref.[39]. The relaxation times of the slowest relaxation are represented by filled grey diamonds in Fig.2, and fitted to the VFT-dependence. The relaxation time data reaches 10^3 s at about 176 K, which defines the dielectric glass transition temperature, T_g, and its value is nearly the same as the glass transition temperature determined by calorimetry as the onset temperature of specific heat of HW in hydrated myoglobin powder (0.4 g/g) shown in Fig.2 of Ref.[34], Fig.2 of Ref.[38] as well as Fig.2 in this paper. The agreement suggests that the slowest process found by NS is the structural α-relaxation of hydrated myoglobin, being associated to the step of specific heat, and its relaxation time can be identified with τ_α.

By inspection of Fig.2 herein, it can be seen that the dielectric α-relaxation from NS remains orders of magnitude slower than the ν-relaxation. The two relaxations have not merged together

at any temperature above T_g shown in Fig.2. Thus, for all temperatures below and above T_g, the fastest dielectric process has to be identified with the ν-relaxation of the HW relaxation. The dielectric τ_ν for various values of h changes temperature dependence from Arrhenius to super-Arrhenius on crossing near either the dielectric or calorimetric T_g. This property is characteristic of the ν-relaxation in aqueous mixtures [4,5,7] and the JG β-relaxation of glass-formers [22], and it is one of several clear evidences that the secondary or ν-relaxation is coupled to the α-relaxation. The fragility index, $m = d\log\tau_\alpha/d(T_g/T)$ had been calculated from the VFT fit to τ_α by NS at $T_g/T=1$ with their $T_g=186.5$ K defined by $\tau_\alpha(T_g)=100$ s. They obtained the value of $m=28.5$ for hydrated myoglobin at $h=0.34$. Such a low value of m is consistent with the calorimetric study by Green et al. [~~55~~62], and indicates that the hydrated protein system are rather "strong" glass-formers as water and various aqueous mixtures [3-5,7]. On the other hand, the VFT dependence in the inset of Fig.2, the equivalent of that constructed in ref. [34], exhibits very rapid increase of the supposedly τ_α of HW on approaching $T_g \approx 173$ K. This proffered property of HW has led Doster [34] to conclude that HW is a highly fragile liquid. The fragility index, $m = d\log\tau_\alpha/d(T_g/T)$ evaluated at $T_g/T=1$ and T_g defined by $\tau_\alpha(T_g)=100$ s, calculated from his VFT fit has the large value of 119, typical of fragile glass-formers. In our previous paper [10], we have already stated that this large value of m of HW is unreasonable. This problem is created when all the relaxation times, including those from the low frequency specific heat spectroscopy, dielectric relaxation, Mössbauer spectroscopy, NMR, and neutron scattering, are all mistakenly collected together and considered all are associated with τ_α. In reality, except for the specific heat spectroscopy data, all relaxation times in the inset of Fig.2 belong to the ν-relaxation of the HW.

Analysis of the dielectric data of myoglobin at $h = 0.34$ by NS [39] shows that the dielectric strength $\Delta\varepsilon_\nu$ of the HW-relaxation (<u>larger </u>open grey diamonds in Fig.2) increase monotonically with increasing temperature at all temperatures and above T_g. These dielectric data from NS correspond to those Doster took in part from Ref.[~~51~~58] at temperatures above T_g, and are shown by the four open black triangles in Fig.2 as well as in the inset. In dielectric spectroscopy, the monotonic increase of the dielectric strength of the HW-relaxation with temperature is the signature of secondary relaxation. On the other hand, it is well known that the dielectric strength of the structural α-relaxation either remains more or less constant or decreases with increasing

temperature. Thus, the major mistake of the construction of the VFT-dependence by the author of ref.[34] has been in combining the dielectric secondary relaxation of HW with the α-relaxation from specific heat spectroscopy. Such a wrong VFT-dependence with a resultant apprent high fragility, shown in the inset of Fig.2, is consequence of not considering additional data that could guide to a more consistent interpretation. As to be shown separately in sections to follow, the temperature dependence of the dielectric strength of the HW-relaxation in hydrated lysozyme [39, 5663] and BSA [5764] also show the signature of a secondary relaxation, and the dielectric relaxation times of this HW relaxation in lysozyme at h=0.4 overlap that from neutron scattering [5663].

Another support of the scenario of the α-relaxation being responsible for the transition at T_d was proffered by Doster Ref.[36] in consideration the wave vector transfer dependence of relaxation time. The statement was made Ref.[36] that "*The relaxation time of hydration water observed with neutron scattering increases with Q as $\tau_c(Q) \sim Q^2$ at low Q, the signature of translational diffusion. The main structural relaxation is thus dominated above 220 K by α-relaxation, local β-processes would exhibit a Q-independent time constant.*". Actually, the observation about the Q-dependence is pertinent indeed, but a more correct statement would be that above 220 K the relaxation observed should not have a localized character. Notwithstanding, this statement of fact does not rule out the ν-relaxation. In fact, the ν-relaxation of HW above T_g is not a local β-relaxation. Unlike the JG β-relaxation of van der Waals molecular or polymeric glass-formers, water in ν-relaxation can translate as well as rotate. At temperatures above T_g, the HW exhibits translational diffusion, and therefore the motion is expected to be non-local and its rotational component is essentially isotropic as found by NMR study [5461]. Furthermore, molecular dynamics simulations by Hong et al. [5865] have found that water undergoes subdiffusive motion from jumps in the short time regime of simulations. There is additional evidence from simulations by Tournier and Smith [5966] that the jumps between minima are activated at temperatures (180–220 K) where the hydration-dependent step change occurs. At 210 K, 75% of the increase over the linear $<u^2>$ is due to the multi-minimum dynamics. Therefore, the jumps observed by simulations show that the HW motion is diffusive and not local *β*-processes as hypothesized by the authors in ref.[36].

The explicit statement was made in another paper of Doster [46]: "*Both processes, termed α and β, in the glass literature (Götze and Sjögren 2005) play a role in hydrated proteins.*". Another paper of his [35] has the title "*The two-step scenario of the protein dynamical transition*". From the statement and the title it is clear that the fast β-process mentioned is the first of the two-step decay of the density correlation function of myoglobin HW in the context of the mode coupling theory (MCT) [37,~~60~~67], which is definitely local because the β-process of MCT is the way MCT uses to describe caging. ~~Actually the β-process of MCT is not even a relaxation process.~~ It is worth pointing out that MCT has β-process of caging and the α-relaxation, but no true secondary relaxation or ν-relaxation in hydrated proteins. Naturally, an explanation based solely on MCT [46, 35] had to rely entirely on the α-relaxation to account for what has been called the PDT. On the other hand, according to us and supported by the simulations of Hong et al. [~~58~~65], caged HW dynamics occurs at times before the secondary ν-relaxation and is observed as the NCL, but it is the ν-relaxation that causes the second step increase of the MSD as demonstrated in Fig.2.

The two vertical arrows at the bottom of Fig.2 indicate values of $1000/T_{on}$ at T_{on}=240 K and 200 K. The higher temperature of 240 K corresponds to the temperature at the second step increase of the mean square displacement measured by IN13 with τ_{res}=140 ps (red horizontal line). The first step increase is always at T_g independent of the energy resolution of the neutron scattering spectrometer. The lower one at 200 K is the onset temperature of the mean square displacement of the heme group in myoglobin crystals, recorded with Mössbauer spectroscopy at τ_{res}=142 ns (green horizontal line). These values were given in Ref.[36]. There is remarkable good agreement of the relaxation time from IN13 neutron scattering (red circles) with τ_{res}=140 ps at T_{on}=240 K as the arrow on the left indicates. The relaxation time from Mössbauer spectroscopy (large black square) is also in agreement with τ_{res}=142 ns as indicated by the arrow on the right. These results additionally confirm that the onset of increase of the mean square displacement is due to the HW ν-relaxation entering or crossing the time window of the spectrometer of neutron scattering or Mössbauer spectroscopy. A better refined model, taking into account the distribution of relaxation time of ν-relaxation and its contribution to the onset of the mean square displacements at T_{on} could be also applied, helping to a more precise

identification and matching of the onset within few degrees, but it is not going to change the scenario.

All the evidences from experiments discussed above point to the process giving rise to the second step increase of the mean square displacement seen by neutron scattering is the water-specific secondary or JG β-relaxation, or the ν-relaxation of the HW, and is definitely not the structural α-relaxation. Therefore, there is no protein dynamics transition according to the definition of Doster, and PDT is a misnomer. The second step increase is simply due to the ν-relaxation entering the time window of the spectrometer, and there is no transition. Our conclusion is similar to the proposition by Frauenfelder and coworkers, that the dynamical transition originates from viscosity-independent β-processes in the hydration shell [40, 6168]. In addition, the onset of translational motions of water molecules corresponding to the ν-relaxation entering the experimental accessible time-window has been recently revealed by MD simulation and NS results [6269].

Hydrated Lysozyme

The interesting question we follow up in consideration is whether hydrated lysozyme and hydrated BSA have similar dynamics as the hydrated myoglobin, and whether we can make the same conclusion on the origin of the so called PDT. The detailed discussion on various issues given above for hydrated myoglobin applies in its entirety to hydrated lysozyme and BSA, and hence we can go directly to the experimental data of these other hydrated proteins. The key fact for hydrated lysozyme at h=0.36 also comes from the recent dielectric data of Nakanishi and Sokolov (NS) [39]. The relaxation times of three processes they found and combined with the data of two processes from a previous work by the same group [5663] are plotted against reciprocal temperature in Fig.3.
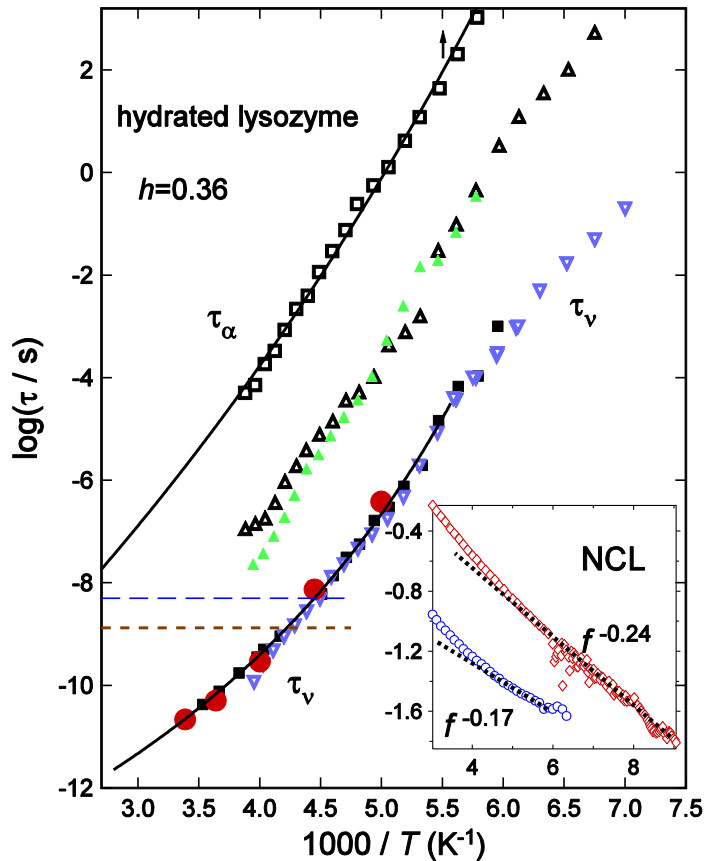
Figure 3. Temperature dependence of the relaxation times of hydrated lysozyme at h =0.36 and All black symbols stand for dielectric relaxation times of three processes obtained by Nakanishi and Sokolov [39]. The green closed triangles and blue inverted triangles are the dielectric relaxation time of two processes found in Ref.[6471]. The large red closed circles present the neutron scattering relaxation times for non-exchangeable protons in protein molecules [6370]. The upper and lower dashed horizontal lines represents the value of τ_v satisfying the condition $\tau_{res}=0.2\tau_v$ and $\tau_{res}=\tau_v$ respectively for the HFBS spectrometer used. The inset is a plot of $\log \varepsilon''$ vs. $\log f$. It shows the nearly constant loss with power law $f^{0.24}$ at 163 K and $f^{0.17}$ at 143 K.

Of the three processes they found, the slowest one has relaxation time with a VFT-dependence, reaching 100 s at 181.5 K, as shown in Fig.3 where the arrow indicate (1000/181.5)=5.5 K^{-1}. This value of glass transition temperature T_g from dielectric relaxation is near the T_g from Brillouin scattering of lysozyme at h=0.40 centered at about 190 K [5663,6370]. The dielectric strength of this process increases with decreasing temperature. All these properties indicate the

slowest relaxation is the structural α-relaxation of the coupled protein and HW system. Its fragility index *m* has the value of 23.7, comparable to 28.5 of the α-relaxation in hydrated myoglobin at *h*=0.34.

On the other hand, the relaxation time of the fastest relaxation changes from an Arrhenius temperature dependence below T_g to a stronger dependence above T_g. They overlap the neutron scattering relaxation times for non-exchangeable protons in lysozyme hydrated with D_2O at *h*=0.4, as obtained using the high-flux backscattering spectrometers (HFBS) at the National Institute of Standards and Technology, with energy resolution of ~ 1μeV [6370]. Its dielectric relaxation strength increases with increasing temperature. All these properties of fastest process are evidence of secondary or ν-relaxation of HW, as concluded before by Khodadadi et al. [6471], and like that in the case of hydrated myoglobin. The lower horizontal line indicates the time resolution of the HFBS neutron scattering spectrometer as done by Khodadadi and Sokolov in Ref.[6572]. The VFT line fitting the combination of dielectric and neutron ν-relaxation times above T_g intersects the time resolution line at *T*=233 K, and this is the temperature at which the second step increase of the MSD occurs if the criterion, $\tau_{res}= \tau_{MAX}=\tau_\nu$ is used. However, this temperature is 225 K (shown by the upper horizontal line) if the criterion, $\tau_{res}=0.2 \, \tau_{MAX} =0.2\tau_\nu$ is adopted. Here, as we mentioned above τ_{MAX} is the most probable relaxation time of the relaxation process, and τ_{res} is the longer experimentally accessible timescale. These two temperature are both consistent with the temperature of the second step increase of the mean square displacement (see Fig.3B in ref.[6572]). Thus it is clear that the second step is due to the ν-relaxation entering the time window of the HFBS, and has nothing to do with either the structural α-relaxation or the PDT as defined in refs.[34-36]. It is noteworthy that a recent dielectric spectroscopy study on frozen lysozyme solutions in water reported, after subtraction of the contribution of ice, a similar scenario for the dielectric relaxation times as reported in hydrated lysozyme [6673].

The inset of Fig.3 shows the nearly constant loss (NCL) found by NS at lower temperatures in the glass state. This is the caged HW dynamics that persists to lower frequencies until it is terminated by the onset of the ν-relaxation. We shall return to discuss this aspect of HW dynamics after presentation of the hydrated BSA data to follow.

20

Hydrated Bovine Serum Albumin

In a previous publication [38] we considered the processes found by dielectric relaxation in hydrated bovine serum albumin (BSA) at h=0.80 and 0.60 taken from the study of Shinyashiki et al. [6774], and calorimetry data of BSA at h=0.80 of Kawai et al. [6875]. Not included are the DSC data of Panagopoulou et al. determining a value of 210 K for T_g of BSA at h=0.20 and other hydration levels [6976]. These important information about the structural α-relaxation are now included into the right panel of Fig.4.
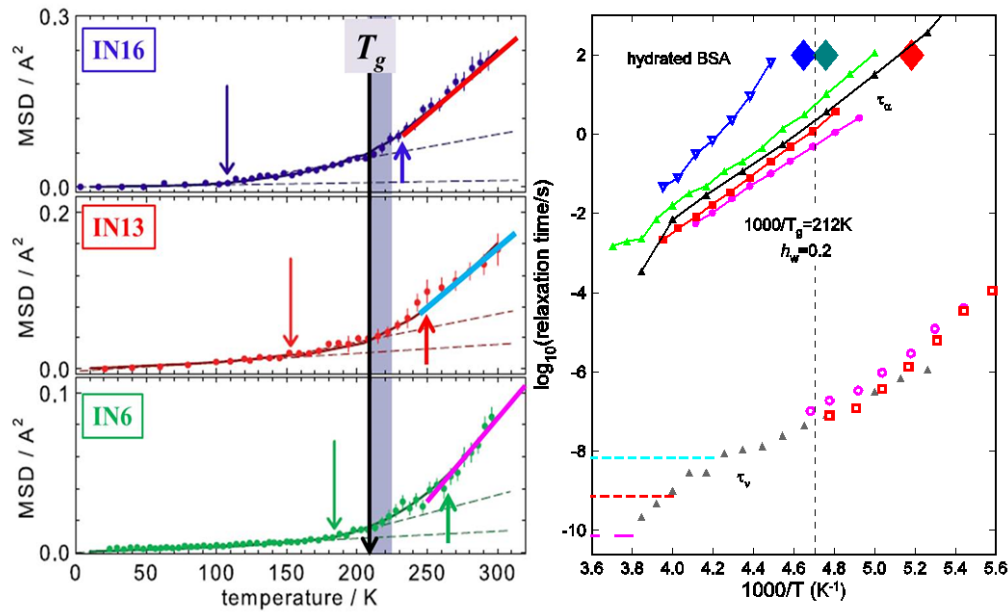

Figure 4. (Left panel): MSD from neutron scattering measurements on IN16, IN13, and IN6 of BSA hydrated at h=0.20 level. Reproduced from Ref.[7077] by permission. Down-pointing arrows define T_{on} the onset rising from their methyl contribution according to Schirò et al. The black vertical arrow indicates T_g=210 K. Red, cyan and magenta lines are regressions drawn respectively for IN16, IN13 and IN6 data. Up-going arrows mark the temperature 233 K, 252 K and 265 K, respectively for IN16, IN13 and IN6 data, matching the points where relaxation times in right panel enters into the experimental windows. (Right panel): Relaxation map of hydrated BSA. The large diamonds on top are values of τ_α from DSC measurements at h=0.18, 0.23, and for h>0.3 from left to right [6976]. The dielectric relaxation times τ_α on top (from left to right) are at h=0.18 (blue inverted triangle), h=0.80 (green triangles), h=0.60 (black triangles), h=0.40 (red closed squares), and h=0.28 (magenta closed circles). Shown below are the dielectric relaxation time τ_ν of the secondary ν-relaxation at h=0.40 (red open squares), h=0.28 (magenta

open circles), and h=0.80 (grey closed triangles). All dielectric data are from Ref.[~~57~~64] except those of BSA at h=0.80 and h=0.60, which are taken from Ref.[~~67~~74]. The horizontal lines are the τ_v=5τ_{res} for IN16, IN13 and IN6 (from top to bottom).

The values of T_g of BSA at h=0.18, 0.23, and 0.30 and greater are 215, 210, and 193 K respectively. The calorimetry data of BSA at h=0.8 from Kawai et al. provides a value of T_g =170 K. Panagopoulou et al. [~~57~~64] made dielectric measurements of hydrated BSA at h=0.18, 0.23, 0.28, and 0.40. Two relaxations were found, and their relaxation times are shown in the right panel of Fig.4. The slower one of two dielectric relaxations has relaxation time longer than 100 s at the DSC T_g of BSA at the same value of h. Its dielectric strength increases with decreasing temperature. Hence it is the structural α-relaxation. The other dielectric relaxation process has relaxation time many orders of magnitude shorter. The data for BSA at h=0.28 and 0.40 from Panagopoulou et al. are reproduced in the right panel of Fig.4 together with that from Shinyashiki et al. at h=0.80. It is the secondary ν-relaxation of HW of BSA with relaxation times τ_v because its dielectric strength increases with increasing temperature.

Schirò et al. [~~70~~77] published neutron scattering measurements on BSA at h=0.20 using three spectrometers, IN6, IN13, and IN16, with widely different energy resolution. The mean square displacement (MSD) obtained are reproduced in the left panel of Fig.4. From their model fit of the data, the methyl group contribution has an onset at temperature T_{on} which depends on the instrument resolution as indicated by the downward pointing arrows on the left panel of Fig.4. Their fit to the data also has another transition occurring within the range of 210 to 215 K, which is independent of instrument resolution. This is the universal step change of MSD at T_g. There is yet another change of slope of the MSD in BSA, which is instrument-resolution dependent at higher temperatures than that occurring near T_g~210 K. Analyzing the MSD data with a numerical procedure [10], it is possible to single out a change to the steeper slope as demonstrated by red, cyan and magenta regression lines drawn respectively for the IN16, IN13 and IN6 data (see left panel in Fig.4). The change at the onset temperature T_{on} is caused by the secondary ν-relaxation of the HW entering into the time window of the spectrometer. Here we use the criterion, τ_{res}=0.2τ_v, to give an independent determination of T_{on} from the temperature dependence of τ_v in the right panel of Fig.4. The dashed lines corresponds to τ_v=5τ_{res}, and the

temperature at which the τ_v data crosses the lines are 233 K, 252 K and 267 K, respectively for τ_{res} of IN16, IN13 and IN6. These values, shown by up-pointing arrows in left panel, are in agreement with the changes of slope determined by linear regression in left panel.

Caged HW Dynamics (NCL)

We mentioned already in the Background that the caged molecules dynamics is a universal feature of the short time dynamics, transpiring at times before the JG β-relaxation. It is manifested as the nearly constant loss (NCL) in susceptibility measured by dielectric relaxation [3,24,26] or dynamic light scattering [25, 32]. The NCL is the loss of the molecules due to motion within the cages formed by the anharmonic intermolecular potential. Since the JG β-relaxation is also intermolecular in nature, its onset effectively dissolves the cages and terminates the NCL regime. This relation between the NCL and the JG β-relaxation has been amply demonstrated by experimental data [24,26,~~71~~78], and rationalized by theoretical considerations [29,26,42-44,~~71~~78]. The intensity of the NCL change to a stronger temperature dependence when temperature is raised to cross T_g from below, reflecting the fact that the caged dynamics and NCL is coupled to density and vitrification. Probed at high frequencies by neutron scattering, the step increase of NCL is observed always at T_g, independent of the energy resolution of the spectrometer.

The NCL has been seen in dielectric spectra of aqueous mixtures [3,10], and some of the properties are found in PVP as shown in Fig.1. In their dielectric study of hydrated lysozyme at h=0.36, Nakanishi and Sokolov found the NCL at temperatures 163 and 143 K, below T_g~181.5 K (see inset of Fig.3). The value of $\log(\tau_v/s)$ is about -4.7 at T_g, which is at least 4.3 decades longer than τ_{res}~10^{-9} s of IN16 and HFBS, and -6.7 decades for IN6. Hence if the methyl group rotation contribution is absent or subtracted, the elastic scattering intensity and the associated MSD contributed by the hydrated lysozyme comes from the NCL of caged HW at temperatures below T_g and somewhat above T_g. The increase of intensity of NCL on crossing is the consequence of the coupling of the caged HW dynamics to density, as in the case of ordinary glass-formers. On further increase of temperature, its contribution is terminated before the onset of the second step change at T_{on} due to the ν-relaxation entering the time window of the

23

spectrometer. In Refs.[10,21,38], we have demonstrated that same properties of the NCL were observed in proteins solvated by saccharides either pure or mixed with water. This was not generally recognized in the literature of the past, and making it known has helped correctly identifying the second step change of the elastic intensity or the MSD to originate from the JG β-relaxation of the solvent coupled to the protein by entering into the time window of the spectrometer.

Molecular dynamics simulations of hydrated lysozyme over the 1 to 100 GHz frequency window by Hong et al. [5865] have found the total susceptibility can be decomposed into three components: the localized diffusion, the methyl group rotations, and the jumps. The fastest process of the three corresponds to the first plateau from 0.3 and up to ~3 ps in the time dependence of the MSD, which is the equivalent of the NCL in the frequency domain. The methyl group rotations, and the thermally activated jumps of HW from one minimum to another follow in time. Thus the results from simulations are in accord with our interpretation of MSD data from neutron scattering in that the first step change comes from the NCL, and the second step change from the ν-relaxation, assuming the methyl group rotation contribution has been subtracted off.

(B) Coupling of Caged Dynamics to JG β-Relaxation in Bioprotectants

Recent studies on the fast dynamics in the glassy state of polyalcohols, pharmaceuticals [41, 42], amorphous polymers [43], van der Waals molecules [44], and metallic alloys [7279] have shown that the caged dynamics appear in susceptibility losses as a frequency power law with a small exponent. It has been also shown that generally the intensity of the fast caged dynamics changes temperature dependence at a temperature T_{HF} nearly coincident with the secondary glass transition temperature $T_{g\beta}$ occurring below the nominal glass transition temperature $T_{g\alpha}$.

The phenomenon and especially the property, $T_{HF} \approx T_{g\beta}$, is remarkable since T_{HF} is determined usually by measurements of fast caged dynamics at short time scales typically in the ns to ps range by neutron scattering and terahertz (THz) dielectric spectroscopy, while $T_{g\beta}$ characterizes the secondary glass transition at which the Johari-Goldstein (JG) β-relaxation time τ_{JG} reaches a long time ~10^3 s, determined directly either by positronium annihilation lifetime

spectroscopy [7380-7683], calorimetry [7784], or low frequency dielectric or mechanical relaxation spectroscopy. The existence of the secondary glass transition originates from the dependence of τ_{JG} on density, previously proven by experiments performed at elevated pressure. The outstanding property of $T_{HF} \approx T_{g\beta}$ follows as consequence of the coupling of the caged dynamics to density as well as coupling to the density dependent JG β-relaxation [24,26,29,33,7178,7885]. The latter originates from the fact that the caged dynamics regime is terminated by the onset of the JG β-relaxation. The density dependence of the caged dynamics or the nearly constant loss (NCL) in susceptibility is amply clear from the step increase of the mean square displacement (MSD) on crossing T_g from the glassy state to the liquid state in all glass-formers including aqueous mixtures and hydrated proteins discussed before in Section (*A*).

The apparent generality of the phenomenon suggested from the results of previous studies on a variety of glass-formers [41,42-44,7279], and particularly the remarkable property, $T_{HF} \approx T_{g\beta}$, imply that the same should be observable in the bio-protectants and proteins embedded in the bio-protectants. In the present paper we present experimental evidences for two di-saccharides, trehalose and sucrose from measurements by neutron scattering to show the step change of the MSD contributed by caged molecules dynamics at T_{HF} below T_g. Dielectric relaxation data are used to obtain the dielectric $T_{g\beta}$. The results make possible either verifying or invalidating the relation $T_{HF} \approx T_{g\beta}$ of these bio-protectants. The results for the monosaccharide glucose and lysozyme embedded in glucose will be published elsewhere.

The source of the THz dielectric spectroscopic data of trehalose we consider in this paper is from Sibik and Zeitler [7986,8087]. The samples have been desiccated and kept in vacuum before measurements. The elastic incoherent neutron scattering data of trehalose and trehalose diluted with 0.05 d8-glycerol are taken from the results published by Cicerone and Soles [8188]. The neutron data of sucrose are from Qian et al. [8289]. The elastic incoherent neutron scattering measurements were performed on the High Flux Backscattering spectrometer (HFBS) at the National Institute of Standards and Technology with energy resolution of 0.85 μeV (FWHM), and the accessible Q range is 0.25–1.75 Å^{-1}.

Trehalose

A comprehensive dielectric relaxation study of the seven disaccharides including trehalose was made by Kaminski et al. [~~83~~90]. The sample was annealed at melting temperature in order to remove water. Observed in trehalose is the α-relaxation in the liquid state, and the two secondary relaxations in the glassy state The faster secondary relaxation (γ) is a common characteristic feature of the entire sugars family (mono-, di-, oligo- and polysaccharide). The molecular origin of this process involves intramolecular degree of freedom as inferred from insensitivity of its relaxation time to pressure found in some mono-saccharides [~~84~~91]. The slower β-relaxation was identified to be intermolecular in origin (*i.e.* a Johari-Goldstein (JG) β-relaxation), involving twisting motion of the mono-sugar rings around the glycosidic bond. The temperature dependences of the relaxation times of the three processes, τ_α, τ_β, and τ_γ are shown in the Arrhenius plot in Fig.5.
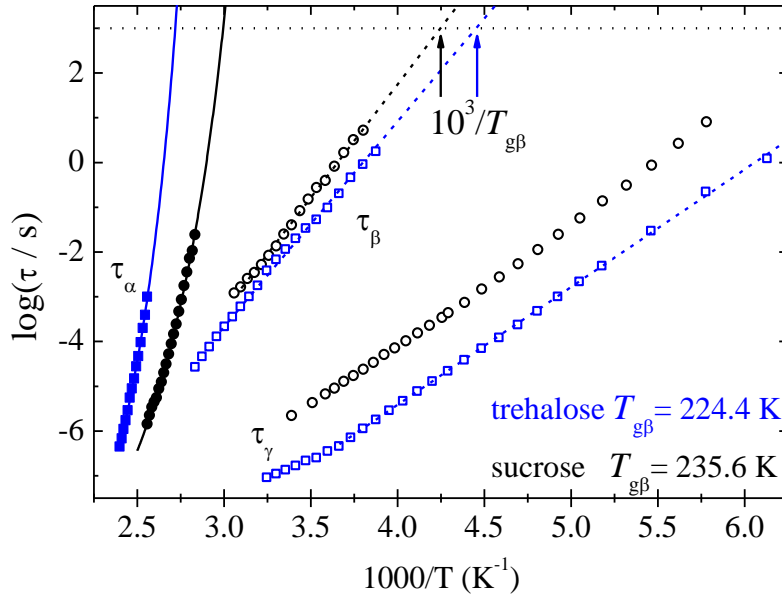
Figure 5. The primary and secondary relaxation times, τ_α, τ_β, and τ_γ (from left to right) of trehalose (blue squares) and sucrose (black circles) from dielectric relaxation measurements shown as a function of reciprocal temperature. The dashed lines are least square fits of τ_β of the two di-saccharides to Arrhenius dependence and extrapolated to longer times to determine the values of $T_{g\beta}$ given in the figure. Horizontal dotted line indicates the isochronal value log (τ/s)=3. Data taken from Ref.[90].

The least square fit of τ_β to Arrhenius dependence in the figure is extrapolated to 1000 s to determine the $T_{g\beta}$=224 K [92]. The same is done for τ_γ to determine $T_{g\gamma}$=137 K, although it may not be physically significant as $T_{g\beta}$ because it is decoupled from density fluctuations. From the extrapolation of the Vogel-Fulcher fit to the dielectric data of τ_α, the value of 371 K was determined for $T_{g\alpha}$. The discrepancy between this dielectric $T_{g\alpha}$ and that given by others has been addressed in ref. [8390].

The Q-dependence of the incoherent elastic neutron scattering intensity I_{inc} from refs.[8188] and [82] was analyzed in terms of the Debye-Waller factor, $I_{inc}(Q)$=exp[-$Q^2<u^2>$/3], where $<u^2>$ is the hydrogen-weighted mean squared displacements (MSD). In Fig.6 we reproduce the temperature dependence of $<u^2>$ in dry and pure trehalose from refs.[8188 8290] together with the data of a freeze dried trehalose glass diluted with d8-glycerol at 0.05 glycerol mass fraction [8188].
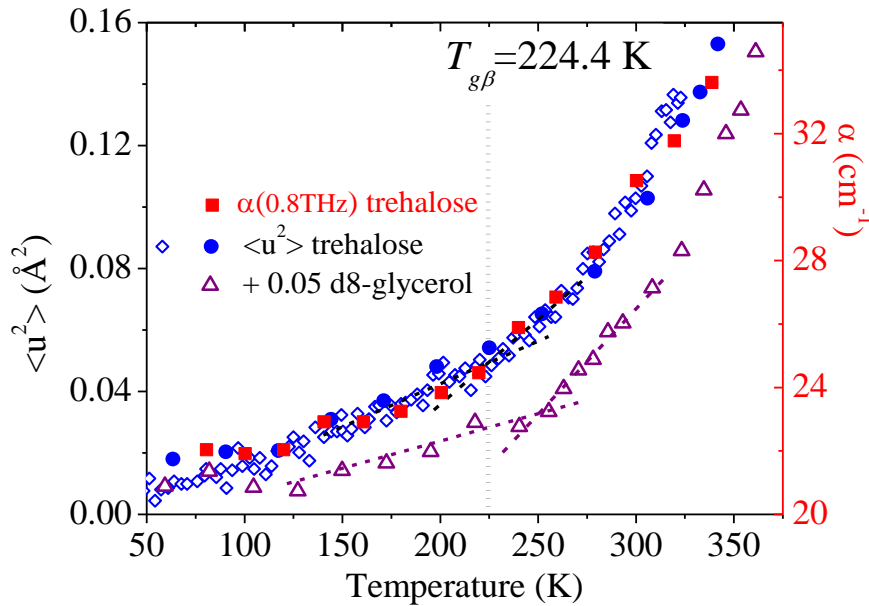

Figure 6. Mean square displacement, $<u^2>$, of trehalose (closed circles) and trehalose mixed with 0.05 wt.% of d-8 glycerol (open triangles) from ref.[8188]. The trehalose data represented by open diamonds are from ref.[8289] after scaling by a factor of 2 to match the data from ref.[8189]. The vertical dotted line is placed at $T_{g\beta}$=224.4 K of trehalose. The dashed lines are drawn to indicate crossover of temperature dependence of $<u^2>$ at T_{HF} nearly coincident with $T_{g\beta}$.

Closed red squares represent Terahertz absorption data of glassy trehalose plotted against temperature from Refs. [~~79~~86] and [~~80~~87]. The scale is on right Y-axis.

The data of Ref.[~~82~~89] of trehalose had been scaled down by a factor of 2 in order to match the data of Ref.[~~81~~88]. The rescaling by a factor 2 perfectly makes sense because in Ref.[~~82~~89] the authors fit their data by $\exp[-Q^2<u^2>/6]$, while in Ref.[~~81~~88] they use $\exp[-Q^2<u^2>/3]$. This operation does not change the temperature dependence of the $<u^2>$ data. The response at short time scales of about 1 ns observed by incoherent elastic scattering in the glassy state of trehalose and trehalose diluted with d8-glycerol in Fig.6 comes from the caged dynamics, as discussed before in Section (A) and from results in Refs.[24,26,29,31,33,42-44, ~~71~~781,~~78~~85]. The two dashed lines are drawn for each case to indicate a change of temperature dependence of $<u^2>$ at T_{HF} located somewhere in the neighborhood of the intersection of the two lines. The vertical dotted line positioned at $T_{g\beta}$=224.4 K of the pure trehalose is near the intersection, and hence the property, $T_{HF}\approx T_{g\beta}$, holds in trehalose. We consider also the data of trehalose diluted with 0.05 mass fraction of d8-glycerol [~~81~~88] because also present is the crossover in temperature dependence of $<u^2>$ at some T_{HF}, somewhat higher than pure trehalose.

The reader may recall in Section A that temperature dependence of $<u^2>$ of hydrated PVP/D_2O or H_2O in Fig.1 and hydrated BSA in Fig.4 does not show the change at any temperature below $T_{g\alpha}$ identifiable with $T_{g\beta}$, in contrast to the observed change in pure trehalose. One reason for this in the case of PVP/D_2O or H_2O is the very few data points taken below $T_{g\alpha}$, automatically preempts detection of the change at below $T_{g\beta}$. Another reason applicable to both cases is the strength of the caged dynamics reflected in the MSD is determined by the anhamonicity of the intermolecular potential, which in turn correlates with the coupling (or non-exponentiality) parameter n of the Coupling Model as shown in Refs.[31,33]. The size of n of the PVP and BSA is reduced by the hydration water. Hence the strength of the caged dynamics of hydrated PVP and BSA becomes weak in the hydrated samples and its change at $T_{g\beta}$ is hard to detect by neutron scattering. Hydration water has very small coupling parameter n [3,7] and is loosely caged. For the same reason as given above, a step change of MSD at the secondary glass transition temperature $T_{g\nu}$, □□□□□□□□□for instance say $\tau_\nu(T_{g\nu})=10^3$ s, is practically impossible to detect experimentally in hydrated proteins.

Terahertz absorption data of trehalose taken between 80 and 340K at 0.8 THz and reported in Refs.[~~79~~86] and [~~80~~87] are reproduced in Fig.6 (right axis). It is worth noting that the absorption data, obtained at frequency of 0.8 THz, show almost the same behavior of $<u^2>$ from neutron scattering, if the Y-axis is suitable rescaled. The crossover of T-dependence of the absorption at some T_{HF} is is practically the same as $T_{g\beta}$, and consistent with that found by by the two intersecting dashed lines from elastic neutron scattering data. It is noteworthy that the two different techniques, probing dynamic observables at different time scales, provide the same transition temperature T_{HF}. This can be easily rationalized in terms of our interpretation of coupling of caged dynamics and $T_{g\beta}$. In fact, the caged dynamics in this range have a NCL power law frequency behavior as $A(T) f^{-c}$ with c positive and much less than 1, with no characteristic time. The amplitude $A(T)$, that mainly contributes to the T-dependence of both $<u^2>$ and THz absorption coefficient in this range, undergoes a transition at $T_{g\beta}$, irrespective on the timescale probed by the spectrometer. The striking correspondence found for the crossover in the same sample by different techniques reinforce our hypothesis that caged dynamics, with NCL behavior, determine the crossover of T-dependence, that it is related to the unfreezing of fluctuations associated to the JG β-relaxation.

Sucrose

Dielectric relaxation study of sucrose has found two secondary relaxations [~~82~~89], the lower one of which is the JG β-relaxation. The relaxation times, τ_β and τ_γ of the two secondary relaxations are shown as a function of reciprocal temperature in Fig.5. The least square fit of the τ_β data by Arrhenius dependence is shown by the line, which has been extrapolated to 10^3 s to determine $T_{g\beta}$=235.6 K, significantly lower than $T_{g\alpha}$=341 K. Elastic scattering intensity of sucrose was measured by the same HFBS neutron spectrometer [81] with the samples cooled from 324 K down to 4 K at 0.7 K per minute, and the data were analyzed to extract $<u^2>$. Fig.7 shows the temperature dependence of $<u^2>$, and the presence of a change of temperature dependence at T_{HF}

as indicated by the intersection of the two lines drawn. The value of T_{HF} is very close to $T_{g\beta}$=235.6 K. The analogy to what observed in ~~glucose~~ threalose is quite strong.
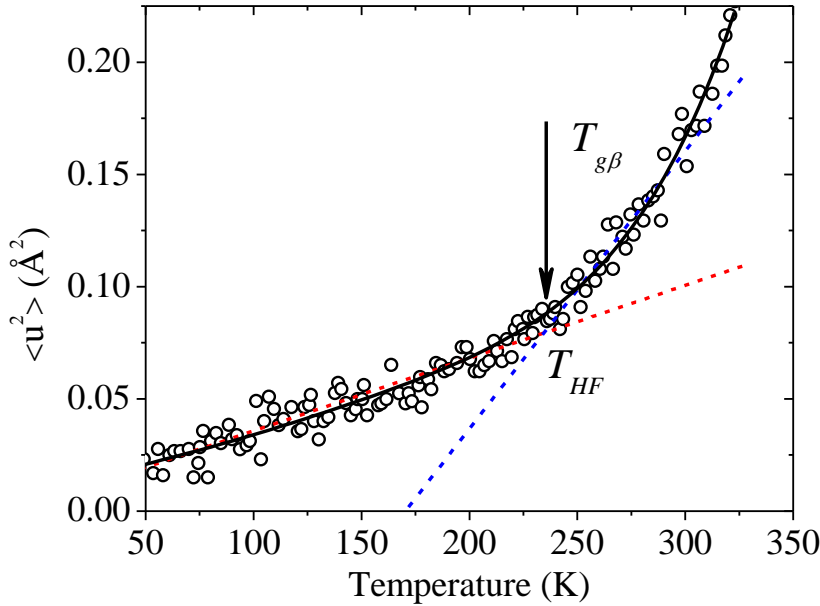

Figure 7. Mean square displacement, $<u^2>$, of sucrose (black open circles) together with the black line to guide the eye from Ref.[~~82~~89]. The vertical arrow is placed at $T_{g\beta}$=235.6 K of sucrose. The red and blue dashed lines are drawn to indicate crossover of temperature dependence of $<u^2>$ at T_{HF} nearly coincident with $T_{g\beta}$.

4. CONCLUSIONS

By amassing experimental data from dielectric relaxation, calorimetry and NMR in three common studied hydrated proteins, myoglobin, lysozyme, and bovine serum albumin, the properties and time scales of three most important processes are completely characterized. They are the caged molecules dynamics, the secondary or ν-relaxation of HW, and the HW-protein

coupled structural α-relaxation, in order of appearance as a function of time. The temperature dependence of relaxation time of the ν-relaxation, $\tau_\nu(T)$, and the α-relaxation, $\tau_\alpha(T)$, are known. The $\tau_\nu(T)$ has Arrhenius temperature dependence below T_g and changes to a stronger T-dependence above T_g. The $\tau_\alpha(T)$ has the VFT dependence but small value of fragility index m, as the mixtures of hydrophilic glass-formers with water, and 'strong' glass-formers. The temperature, T_{on}, at which $\tau_\nu(T)$ enters the time window of Mössbauer spectroscopy and the neutron scattering spectrometer used is determined, and corresponds well to the temperature T_d where step change of either the mean square displacement $<u^2(T)>$ or the elastic scattering intensity is observed. The latter has been dubbed the protein dynamical transition (PDT). On the other hand, at $T=T_d$, $\tau_\alpha(T_d)$ is much longer than $\tau_\nu(T_d)$ by orders of magnitude, and thus the α-relaxation cannot be responsible for the PDT in all three hydrated proteins. Reached completely from experimental evidences, our conclusion rules out the thesis that the PDT originates from the structural α-relaxation and viscous flow. As the way it is defined by Doster, the term PDT is thus a misnomer and should not be used anymore. Previous works by other associating the importance of the PDT to biological functions should now be attributed to the onset of the ν-relaxation of HW. Although different in details, our interpretation is consistent with those of Frauenfelder and coworkers [40, 6168], and also Sokolov and coworkers [39, 5562, 6370, 6471].

Moreover, exact analogue of the PDT is found in the bulk of mixture of polyvinylpyrrolidone (PVP) with 40 wt.% water, and is also caused by the ν-relaxation entering the time window of the neutron scattering spectrometer. This example shows that the effect is general and not restricted to hydrated protein, and thus a new term is needed to describe it instead of PDT.

If the methyl group rotation contribution is removed, we have shown before that the first step change of the $<u^2(T)>$ or the elastic scattering intensity observed at $T_{g\alpha}$ originates from the caged dynamics (or NCL) of the HW [38] or the bio-protectant with or without additional water [21]. This first step change was not recognized as such before in some studies, resulting in wrong interpretations. Now there is direct experimental evidence of the NCL in the glassy state of hydrated lysozyme to support our interpretation.

The coupling of the NCL to the JG β-relaxation has manifested itself as a step change of the NCL at the secondary transition temperature $T_{g\beta}$ observed by terahertz absorption spectroscopy and neutron scattering. This is apparently a general phenomenon because it has been found in the polyalcohols, several pharmaceuticals, a number of amorphous polymers, and van der Waals molecular glass-formers. We have demonstrated that the same effect is found in bio-protectants including trehalose and sucrose. Preliminary studies of glucose and lysozyme embedded in glucose have found the same effect. These findings may have positive impact in understanding the mechanisms preventing degradation of proteins when embedded in glassy bio-protectants.

5. GENERAL SIGNIFICANCE

According to a line of thought maintained steadfastly in the literature by Doster, the so-called protein dynamical transition (PDT) of hydrated proteins is caused by the structural α-relaxation of the protein coupled to HW entering the time windows of Mössbauer spectroscopy and neutron scattering occurring at temperature T_d, some few tens of degrees above $T_{g\alpha}$ dependent on the energy resolution of the instrument. On the other we had interpreted the step change of the mean square displacement or the elastic scattering intensity at T_d originates from the secondary or ν-relaxation of HW entering the instrument time windows. In this paper we have assembled all experimental evidences available at the present time from our data and that of others in literature to show unequivocally that the PDT cannot be caused by the structural α-relaxation, and instead it originates from the ν-relaxation of hydration water (HW). The result settles the long-running controversy on the nature of the PDT, and indicates that the term PDT is a misnomer.

On a separate issue we have used direct experimental evidence of the nearly constant loss (NCL) of caged molecules dynamics to support our interpretation of the first step change of the mean square displacement at $T_{g\alpha}$ as originating from the coupling of the caged molecules dynamics to density and response to vitrification. In many different but ordinary glass-formers, the caged molecules dynamics is also coupled to the JG β-relaxation and the coupling is reflected by a step change of the NCL observed by terahertz absorption spectroscopy and neutron

scattering at the secondary glass transition temperature $T_{g\beta}$. We found the same effect in several bio-protectants and preliminary data indicates the same in lysozyme embedded in glucose.

References

[1] E. J. Sutter and C. A. Angell, Glass Transitions in Molecular Liquids. I. Influence of Proton Transfer Processes in Hydrazine-Based Solutions, J. Phys. Chem. 75 (1971) 1826.

[2] A. Minoguchi, R. Richert, and C. A. Angell, Dielectric Relaxation in Aqueous Solutions of Hydrazine and Hydrogen Peroxide: Water Structure Implications, J. Phys. Chem. B 108 (2004) 19825-19830.

[3] S. Capaccioli, and K. L. Ngai, Resolving the controversy on the glass transition temperature of water? J. Chem. Phys. 135 (2011) 104504.

[4] N. Shinyashiki, S. Sudo, S. Yagihara, A. Spanoudaki, A. Kyritsis, and P. Pissis, Relaxation processes of water in the liquid to glassy states of water mixtures studied by broadband dielectric spectroscopy, J. Phys.: Condens. Matter 19 (2007) 205113.

[5] S.Capaccioli, K.L. Ngai, N. Shinyashiki, The Johari-Goldstein β-relaxation of water. J Phys Chem B. 111 (2007) 8197–209.

[6] S. Cerveny, G.A. Schwartz, A. Alegria, R. Bergman, J. Swenson, Water dynamics in n-propylene glycol aqueous solutions, J. Chem. Phys. 124 (2006) 194501.

[7] K. L. Ngai, S. Capaccioli, S. Ancherbak, and N. Shinyashiki, Philos. Mag. 91 (2011) 1809.

[8] Y. Hayashi, A. Puzenko, I. Balin, Y.E. Ryabov,Y. Feldman, J. Phys.Chem. B 109 (2005) 917.

[9] T. Psurek, S. Maslanka, M. Paluch, R. Nozaki, K.L. Ngai, Effects of water on the primary and secondary relaxation of xylitol and sorbitol: Implication on the origin of the Johari-Goldstein relaxation, Phys.Rev. E   70 (2004) 011503.

[10] K.L. Ngai, S. Capaccioli, A. Paciaroni, Nature of the water specific relaxation in hydrated proteins and aqueous mixtures, Chemical Physics 424 (2013) 37–44.

[11] S. E. Pagnotta, S. Cerveny, A. Alegría, and J. Colmenero, Dielectric relaxations in ribose and deoxyribose supercooled water solutions, J. Chem. Phys. 131 (2009) 085102.

[12] S.K. Jain,G.P. Johari, Dielectric Studies of Molecular Motions In the Glassy States of Pure and Aqueous Poly (vlnylpyrrolldone), J. Phys.Chem. 92 (1988) 5851.

[13] M. Tyagi, S.S.N. Murthy, Dynamics of water in supercooled aqueous solutions of glucose and poly(ethylene glycol)s as studied by dielectric spectroscopy, Carbohydr. Res. 341 (2006) 650.

[14] S. Cerveny, A. Alegria, J. Colmenero, Broadband dielectric investigation on poly„vinyl pyrrolidone and its water mixtures, J. Chem. Phys. 128 (2008) 044901.

[15] R. Busselez, A. Arbe, S. Cerveny, S. Capponi, J. Colmenero, B. Frick, Broadband dielectric investigation on poly„vinyl pyrrolidone and its water mixtures, J. Chem. Phys. 137 (2012) 084902.

[16] K. Pathmanathan, G.P. Johari, Dielectric and Conductivity relaxation in Poly(HEMA) and of Water in its Hydrogel, J. Polym. Sci., Part B: Polym.Phys., 28 (1990) 675.

[17] K. Pathmanathan, G.P. Johari, Relaxation and Crystallization of Water in a Hydrogel , J. Chem. Soc. Faraday Trans., 90 (1994) 1143.

[18] N. Shinyashiki, M. Shinohara, Y. Iwata, T. Goto, M. Oyama, S. Suzuki, W. Yamamoto, S. Yagihara, T. Inoue, S. Oyaizu, S. Yamamoto, K. L. Ngai, and S. Capaccioli, The Glass Transition and Dielectric Secondary Relaxation of Fructose-Water Mixtures, J. Phys. Chem. B 112 (2008) 15470–15477

[19] S. Magazu, F. Migliardo, and M. T. F. Telling, Study of the dynamical properties of water in disaccharide solutions, Eur. Biophys. J. 36 (2007) 163–171.

[20] S. E. Pagnotta, A. Alegria, and J. Colmenero, Dynamical behavior of highly concentrated trehalose water solutions: a dielectric spectroscopy study, Phys. Chem. Chem. Phys. 14 (2012) 2991–2996.

[21] S. Capaccioli, K.L. Ngai, S. Ancherbak, A. Paciaroni, Evidence of Coexistence of Change of Caged Dynamics at T_g and the Dynamic Transition at T_d in Solvated Proteins, J. Phys. Chem. B 116 (2012) 1745.

[22] K.L. Ngai, M. Paluch, Classification of Secondary Relaxation in Glass-Formers Based on Dynamic Properties, J. Chem. Phys. 120 (2004) 857.

[23] G.P. Johari, M. Goldstein, Viscous Liquids and the Glass Transition. II. Secondary Relaxations in Glasses of Rigid Molecules, J.Chem.Phys. 53 (1970) 2372-2388.

[24] K.L. Ngai, An extended coupling model description of the evolution of dynamics with time in supercooled liquids and ionic conductors, J. Phys.: Condens. Matter 15 (2003) S1107–S1125.

[25] A.P. Sokolov, A Kisliuk, V.N. Novikov, K.L. Ngai, Observation of constant loss in fast relaxation spectra of polymers, Phys. Rev. B 63 (2001) 172204.

[26] S. Capaccioli, M. Shahin Thayyil, and K. L. Ngai, Critical Issues of Current Research on the Dynamics Leading to Glass Transition, J. Phys. Chem. B, 112 (2008) 16035-16049.

[27] K. L. Ngai and S. Capaccioli, Unified explanation of the anomalous dynamic properties of highly asymmetric polymer blends, J. Chem. Phys. 138 (2013) 054903.

[28] K. L. Ngai and S. Capaccioli, Reconsidering the Dynamics in Mixtures of Methyltetrahydrofuran with Tristyrene and Polystyrene, J. Phys. Chem. B 119 (2015) 5677−5684.

[29] K. L. Ngai, Why the fast relaxation in the picosecond to nanosecond time range can sense the glass transition, Philos. Mag. 84 (2004) 1341.

[30] S. Kastner, M. Köhler, Y. Goncharov, P. Lunkenheimer, A. Loidl, High-frequency dynamics of type B glass formers investigated by broadband dielectric spectroscopy, J.Non-Cryst. Solids 357 (2011) 510–514.

[31] K.L. Ngai, Dynamic and thermodynamic properties of glass-forming substances, J. Non-Cryst. Solids 275 (2000) 7-51.

[32] A. Kisliuk, V.N. Novikov, A.P. Sokolov, Constant loss in Brillouin spectra of polymers, J. Polym. Sci., Part B: Polym. Phys., 40 (2002) 201.

[33] K.L. Ngai, Relaxation and Diffusion in Complex Systems; Springer: New York; (2011).

[34] W. Doster, The protein-solvent glass transition, Biochimica et Biophysica Acta 1804 (2010) 3–14.

[35] W. Doster, The two-step scenario of the protein dynamical transition, J. Non-Cryst. Solids 357 (2011) 622.

[36] W. Doster, H. Nakagawa, and M. S. Appavou, Scaling analysis of bio-molecular dynamics derived from elastic incoherent neutron scattering experiments, J. Chem. Phys. 139 (2013) 045105.

[37] W. Götze, Complex dynamics of glass-forming liquids, International Series of Monographs on Physics 143, Oxford Science Publications, (2009).

[38] K. L. Ngai, S. Capaccioli, and A. Paciaroni, Change of caged dynamics at T_g in hydrated proteins: Trend of mean squared displacements after correcting for the methyl-group rotation contribution, J. Chem. Phys. 138 (2013) 235102.

[39] M. Nakanishi, A. P. Sokolov, Protein dynamics in a broad frequency range: Dielectric spectroscopy studies, J. Non-Cryst. Solids, 407 (2015) 478–485.

[40] H. Frauenfelder, G. Chen, J. Berendsen, P.W. Fenimore, H. Jansson, B.H. McMahon, I.R. Stroe, J. Swenson, R.D. Young, A unified model of protein dynamics, Proc. Natl. Acad. Sci. 106 (2009) 5129–5134.

[41] J. Sibik, S.R. Elliott, J.A. Zeitler, Thermal Decoupling of Molecular-Relaxation Processes from the Vibrational Density of States at Terahertz Frequencies in Supercooled Hydrogen-Bonded Liquids, J. Phys. Chem. Lett. 5 (2014) 1968−1972.

[42] S. Capaccioli, K. L. Ngai, M. Shahin Thayyil, D. Prevosto, Coupling of Caged Molecule Dynamics to JG β-Relaxation: I, J. Phys. Chem. B 119 (2015) 8800–8808.

[43] K. L. Ngai, S. Capaccioli, D. Prevosto, Li-Min Wang, Coupling of Caged Molecule Dynamics to JG β-relaxation II: Polymers, J. Phys. Chem. B 119 (2015) 12502 .

[44] K. L. Ngai, S. Capaccioli, D. Prevosto, Li-Min Wang, Coupling of Caged Molecule Dynamics to JG β-relaxation III: van der Waals Glasses, J. Phys. Chem. B, 119 (2015) 12519.

[45] H. Lichtengegger, W. Doster, Th. Kleinert, A. Birk, B. Sepiol, G. Vogl, Heme-solvent coupling, a Mössbauer study of myoglobin in sucrose, Biophys. J. 76 (1999) 414–422.

[46] W. Doster, The dynamical transition of proteins, concepts and misconceptions, Eur. Biophys. J. 37 (2008) 591−602.

[47] W. Doster, M. Settles, Protein–water displacement distributions, Biochim. Biophys. Acta 1749 (2005) 173–186.

[48] G. U. Nienhaus, H. Frauenfelder, F. Parak, Structural fluctuations in glass-forming liquids: Mossbauer spectroscopy on iron in glycerol, 41 (1991) 3345-3350.

[49] M. Jasnin, L. van Eijck, M. Marek Koza, J. Peters, C. Laguri, H. Lortat-Jacob, G. Zaccai, Phys. Chem. Chem. Phys. Dynamics of heparan sulfate explored by neutron scattering, 12 (2010) 3360-3362.

[50] T. Becker, J. A. Hayward, J. L. Finney, R. M. Daniel and J. C. Smith, Neutron Frequency Windows and the Protein Dynamical Transition, Biophys. J., 2004, 87, 1436-1443.

[51] K. L. Ngai, S. Capaccioli, S. Ancherbak, N. Shinyashiki, Resolving the ambiguity of the dynamics of water and clarifying its role in hydrated proteins, Philosophical Magazine, 91 (2010) 1809-1835.

[52] Salvatore Magazù, Federica Migliardo, Antonio Benedetto, Puzzle of Protein Dynamical Transition, J. Phys. Chem. B, 115 (2011) 7736-7742.

[53] Salvatore Magazù, Federica Migliardo, and Antonio Benedetto, Elastic incoherent neutron scattering operating by varying instrumental energy resolution: Principle, simulations, and experiments of the resolution elastic neutron scattering (RENS), Review of Scientific Instruments 82 (2011) 105115-1-11.

[54] S. Magazù, F. Migliardo, M. T. Caccamo, Advances in Materials Science and Engineering, Volume 2013 (2013), Article ID 695405, http://dx.doi.org/10.1155/2013/695405].

[55] F.G. Parak, and G. U. Nienhaus, Glass-like behaviour of proteins as seen by Mössbauer spectroscopy, J. Non-Cryst. Solids, 131-133 (1991) 362-368.

[4956] F. G. Parak, K. Achterhold, S. Croci. M. Schmidt, A Physical Picture of Protein Dynamics and Conformational Changes, J. Biol. Phys. 33 (2007) 371–387.

[5057] R.D. Young, H. Frauenfelder, P.W. Fenimore, Phys. Rev. Lett. 107 (2011) 158102-1-02-4.

[5158] J. Swenson, H. Jansson, R. Bergman, Relaxation processes in super-cooled and confined water and implications for protein dynamics, Phys. Rev. Lett. 96 (2006) 247802–247804.

[592] H. Jansson, R. Bergman and J. Swenson, Relation between Solvent and Protein Dynamics as Studied by Dielectric Spectra, J. Phys. Chem. B 109 (2005) 24134.

[6053] H. Jansson and J. Swenson, The protein glass transition as measured by dielectric spectroscopy and differential scanning calorimetry, Biochim. Biophys. Acta 1804 (2010) 20.

[6154] S. A. Lusceac, M. R. Vogel, C. R. Herbers, ^{2}H and ^{13}C NMR studies on the temperature-dependent water and protein dynamics in hydrated elastin, myoglobin and collagen, Biochim. Biophys. Acta 1804 (2010) 41.

[6255] J.L. Green, J. Fan, C.A. Angell, The protein-glass analogy: new insight from homopeptide comparisons, J. Phys. Chem. 98 (1994) 13780–13790.

[6356] S. Khodadadi, S. Pawlus, J. H. Roh, V. Garcia Sakai, E. Mamontov, and A. P. Sokolov, The origin of the dynamic transition in proteins, J. Chem. Phys. 128 (2008) 195106.

[6457] A. Panagopoulou, A. Kyritsis, N. Shinyashiki, and P. Pissis, Protein and Water Dynamics in Bovine Serum Albumin−Water Mixtures over Wide Ranges of Composition, J. Phys. Chem. B 116 (2012) 4593−4602

[6558] L. Hong, N. Smolin, B. Lindner, A. P. Sokolov, and J. C. Smith, Three Classes of Motion in the Dynamic Neutron-Scattering Susceptibility of a Globular Protein, Phys. Rev. Lett 107 (2011) 148102.

[6659] A. L. Tournier and J. C. Smith, Principal Components of the Protein Dynamical Transition, Phys. Rev. Lett. 91 (2003) 208106.

[670] W. Götze, L. Sjögren, Relaxation processes in supercooled liquids, Rep. Prog. Phys. 55 (1992) 241–376.

[681] P. W. Fenimore, H. Frauenfelder, S. Magazù, B. H. McMahon, F. Mezei, F. Migliardo, R. D. Young, I. Stroe, Concepts and problems in protein dynamics, Chemical Physics 424 (2013) 2–6.

[692] G. Schirò, Y. Fichou, F.s-X. Gallat, K. Wood, F. Gabel, M. Moulin, M. Hartlein, M. Heyden, J.-P. Colletier, A. Orecchini, A. Paciaroni, J. Wuttke, D. Tobias, M. Weik, Translational diffusion of hydration water correlates with functional motions in folded and intrinsically disordered proteins. Nature Communications 6 (2015) 6490.

[6370] S. Khodadadi, A. Malkovskiy, A. Kisliuk and A. P. Sokolov, A broad glass transition in hydrated proteins, Biochim. Biophys. Acta, 1804 (2010) 15–19.

[6471] S. Khodadadi, S. Pawlus, and A. P. Sokolov, Influence of Hydration on Protein Dynamics: Combining Dielectric and Neutron Scattering Spectroscopy Data, J. Phys. Chem. B 112 (2008) 14273–14280.

[6572] S. Khodadadi, and A. P. Sokolov, Protein dynamics: from rattling in a cage to structural relaxation, Soft Matter, 11 (2005) 4984.

[6673] M. Wolf, S. Emmert, R. Gulich, P. Lunkenheimer, and A. Loidl, Dynamics of protein hydration water, Phys. Rev. E 92 (2015) 032727.

[6774] N. Shinyashiki, W. Yamamoto, A. Yokohama, T. Toshihari, S. Yagihara, R. Kita, K.L. Ngai, and S. Capaccioli, Glass Transitions in Aqueous Solutions of Protein (Bovine Serum Albumin), J. Phys. Chem. B. 113 (2009) 14448.

[6875] K. Kawai, T. Suzuki, and M. Oguni, Low-Temperature Glass Transitions of Quenched and Annealed Bovine Serum Albumin Aqueous Solutions Biophys. J. 90 (2006) 3732.

[6976] A. Panagopoulou, A. Kyritsis, R. Sabater Serra, J.L. Gómez Ribelles, N. Shinyashiki, P. Pissis, Glass transition and dynamics in BSA–water mixtures over wide ranges of composition

studied by thermal and dielectric techniques, Biochimica et Biophysica Acta 1814 (2011) 1984–1996.

[7077] G. Schirò, F. Natali, A. Cupane, Physical Origin of Anharmonic Dynamics in Proteins: New Insights From Resolution-Dependent Neutron Scattering on Homomeric Polypeptides, Phys. Rev. Lett. 109 (2012) 128102.

[7178] K. L. Ngai, Interpreting the nonlinear dielectric response of glass-formers in terms of the coupling model, J. Chem. Phys. 142, 114502 (2015).

[7292] Z. Wang, K. L. Ngai, W. H. Wang, S. Capaccioli, Coupling of caged molecule dynamics to JG β-relaxation in metallic glasses, J. Appl. Phys. in press (2016).

[8073] H. A. Hristov, B. Bolan, A.F. Yee, L. Xie, D.W. Gidley, Measurement of Hole Volume in Amorphous Polymers Using Positron Spectroscopy, Macromolecules 29 (1996) 8507-8516.

[8174] C. L. Wang, T. Hirade, F.H.J. Maurer, M. Eldrup, N.J. Pedersen, Free-Volume Distribution and Positronium Formation in Amorphous Polymers: Temperature and Positron-Irradiation-Time Dependence, J. Chem. Phys 108 (1996) 4654.

[8275] N. Qi, Z.Q. Chen, A. Uedono, Molecular Motion and Relaxation below Glass Transition Temperature in Poly(Methyl Methacrylate) Studied by Positron Annihilation, Radiation Physics and Chemistry, 108 (2015) 81–86.

[8376] J. Bartoš, O. Šauša, G.A. Schwartz, A. Alegría, J.M. Alberdi, A. Arbe, J. Krištiak, J. Colmenero, Positron Annihilation and Relaxation Dynamics from Dielectric Spectroscopy and Nuclear Magnetic Resonance: Cis-trans-1,4-poly(butadiene), J. Chem. Phys. 134 (2011) 164507.

[8477] M. Hatase, M. Hanaya, T. Hikima, M. Oguni, Discovery of Homogeneous-Nucleation-Based Crystallization in Simple Glass-Forming Liquid of Toluene below its Glass-Transition Temperature, J. Non-Cryst. Solids 307–310 (2002) 257–263.

[8578] K. L. Ngai, in Slow Dynamics in Complex Systems: 3rd International Symposium, edited by Tokuyama M. and Oppenheim, I., AIP Conf. Proc. 708 (2004) 515.

[8679] J. Sibik, and J. A. Zeitler, Terahertz Response of Organic Amorphous Systems: Experimental Concerns and Perspectives, Philos.Mag. (2015), DOI: 10.1080/14786435.2015.1111528.

[870] J. Sibik, J.A. Zeitler, Terahertz Dynamics of Amorphous (Bio)Pharmaceutical Mixtures, 2015, Conference "IRMMW-THz-2015, 40th International Conference on Infrared, Millimeter,

and Terahertz Waves", Proceedings available at http://vigir.missouri.edu/~gdesouza/Research/Conference_CDs/IRMMW-THz-2015/.

[881] M. T. Cicerone, C. L. Soles, Fast Dynamics and Stabilization of Proteins: Binary Glasses of Trehalose and Glycerol, Biophys. J. 86 (2004) 3836–3845.

[892] K.K. Qian, P.J. Grobelny, M. Tyagi, M.T. Cicerone, Using the Fluorescence Red Edge Effect to Assess the Long-Term Stability of Lyophilized Protein Formulations, Mol. Pharmaceutics 12 (2015)1141−1149.

[9083] K. Kaminski, E. Kaminska, P. Wlodarczyk, S. Pawlus, D. Kimla, A. Kasprzycka, M. Paluch, J. Ziolo, W. Szeja, K.L. Ngai,; Dielectric Studies on Mobility of the Glycosidic Linkage in Seven Disaccharides, J. Phys. Chem. B 112 (2008) 12816–12823.

[9184] K. Kaminski, E. Kaminska, P. Wlodarczyk, M. Paluch, J. Ziolo, K.L. Ngai, Dielectric Relaxation Study of the Dynamics of Monosaccharides: D-ribose and 2-Deoxy-D-Ribose, J. Phys.: Condens. Matter 20 (2008) 335104.

[92] In studies by dielectric spectroscopy, some workers use either 100 or 1000 s for the relaxation time to reach at the glass transition temperature. The difference in the value of the glass transition temperature is not large. For $T_{g\beta}$ we use 1000 s in conformity with previous publications on the same topic in Refs.[42-44].